



PROCEEDINGS OF THE ELEVENTH ANNUAL ACQUISITION RESEARCH SYMPOSIUM

THURSDAY SESSIONS VOLUME II

A Robust Design Approach to Cost Estimation: Solar Energy for Marine Corps Expeditionary Operations

Susan Sanchez, Naval Postgraduate School
Matthew M. Morse, United States Marine Corps
Stephen Upton, Naval Postgraduate School
Mary L. McDonald, Naval Postgraduate School
Daniel A. Nussbaum, Naval Postgraduate School

Published April 30, 2014

Approved for public release; distribution is unlimited.

Prepared for the Naval Postgraduate School, Monterey, CA 93943.



The research presented in this report was supported by the Acquisition Research Program of the Graduate School of Business & Public Policy at the Naval Postgraduate School.

To request defense acquisition research, to become a research sponsor, or to print additional copies of reports, please contact any of the staff listed on the Acquisition Research Program website (www.acquisitionresearch.net).



ACQUISITION RESEARCH PROGRAM
GRADUATE SCHOOL OF BUSINESS & PUBLIC POLICY
NAVAL POSTGRADUATE SCHOOL

Panel 22. Enhancing Cost Estimating Techniques

Thursday, May 15, 2014	
3:30 p.m. – 5:00 p.m.	<p>Chair: Daniel A. Nussbaum, Naval Postgraduate School, former Director, Naval Center for Cost Analysis</p> <p><i>A Robust Design Approach to Cost Estimation: Solar Energy for Marine Corps Expeditionary Operations</i></p> <p>Susan Sanchez, Naval Postgraduate School Matthew M. Morse, United States Marine Corps Stephen Upton, Naval Postgraduate School Mary L. McDonald, Naval Postgraduate School Daniel A. Nussbaum, Naval Postgraduate School</p> <p><i>The Budding SV3: Estimating the Cost of Architectural Growth Early in the Life Cycle</i></p> <p>Matthew Dabkowski, U.S. Army/University of Arizona Ricardo Valerdi, University of Arizona</p> <p><i>Using Cost Estimating Relationships to Develop A Price Index for Tactical Aircraft</i></p> <p>Stanley Horowitz, Institute for Defense Analyses Bruce Harmon, Institute for Defense Analyses Daniel Levine, Institute for Defense Analyses</p>



A Robust Design Approach to Cost Estimation: Solar Energy for Marine Corps Expeditionary Operations

Susan M. Sanchez—is a professor of operations research at the Naval Postgraduate School, and co-director of NPS's *Simulation Experiments & Efficient Designs (SEED) Center for Data Farming*. She also holds a joint appointment in the Graduate School of Business & Public Policy. Her research interests include the design and analysis of large-scale simulation experiments, with applications in military operations, business, quality, manufacturing, and health care. She has long been active in the simulation community, including the Winter Simulation Conference's Board of Directors, and the American Statistical Association's Section on Statistics in Defense and National Security. [ssanchez@nps.edu]

Matthew M. Morse—is a logistics officer in the United States Marine Corps. He holds a BS in systems engineering from the U.S. Naval Academy and an MS in business administration from Boston University. He is currently serving as a graduate student in the Modeling, Virtual Environments and Simulation (MOVES) curriculum at the Naval Postgraduate School (Monterey, CA). Capt Morse's thesis research assesses the robustness of the HOMER model for Marine Corps Expeditionary Operations under the guidance of Dr. Dan Nussbaum. [mmmorse@nps.edu]

Stephen C. Upton—is a research faculty associate for the Simulation Experiments and Efficient Designs (SEED) Center for Data Farming at the U.S. Naval Postgraduate School (Monterey, CA). He earned his Master of Science degrees in operations research and physics from the Naval Postgraduate School and his Bachelor of Science degree in physics from the University of Idaho. He served 24 years on active duty with the U.S. Marine Corps. His research includes application of high performance computing to simulation experiments, evolutionary computation, and agent-based simulations and their application in studying complex adaptive defense systems. [scupton@nps.edu]

Mary L. McDonald—is a research faculty associate for the Simulation Experiments and Efficient Designs (SEED) Center for Data Farming at the U.S. Naval Postgraduate School (Monterey, CA). She earned her Master of Science degree in applied mathematics from the Naval Postgraduate School and her Bachelor of Arts degree in mathematics from Northwestern University. Her research interests include complex adaptive systems, agent-based modeling, the application of evolutionary algorithms to simulation, and the dynamics of co-evolution. [mlmcdona@nps.edu]

Daniel A. Nussbaum—teaches courses in cost estimating and analysis, mentors students throughout their graduate coursework, including their master's theses, provides Cost Estimating and Business Case Analyses for DoD organizations such as Department of Navy, Department of Air Force, Department of Army, and the Office of Secretary of Defense. He designs, develops, and delivers distance learning courses in cost estimating and analysis, especially the world's only all-distance learning Master's in Cost Estimating and Analysis. He chairs the NPS Energy Academic Group, and provides leadership to SECNAV Executive Energy Education program.

Abstract

Life Cycle Cost (LCC) assessments are of interest during the design phase for new systems. These often involve costs that must be estimated from a variety of different sub-models, including cost models constructed from historical data, forecast models that attempt to predict future economic conditions, and economy-of-scale models that impact production schedules, and more. When these disparate models are put together to obtain an overall cost model, many of these individual sources of uncertainty end up being aggregated or ignored. Consequently, the cost estimates may not provide program managers with appropriate assessments of the risk and overall variability of the new systems. We propose a structured approach for obtaining robust LCC estimates by taking into account a broad set of environmental noise conditions. This will enable program managers to better understand the uncertainty in their overall estimates, and to identify any decision factor combinations that result in both low costs and low cost variability. This may provide guidance on which of the many potential uncertainty sources require close monitoring, and which can safely be



disregarded. We illustrate this approach with a model that the USMC is evaluating for use in cost/benefit analysis of alternative energy systems.

Introduction

Taguchi made a major contribution to the quality engineering literature through his vision of building quality into the product at the manufacturing design level (Taguchi, 1986, 1987; Taguchi & Wu, 1980). He recognized that a careful choice of settings for design *decision factors* (or *parameters*) could lead to products that were insensitive to uncertainties in the manufacturing and customer environment. The uncertainties, or *noise factors* were uncontrollable (or controllable only at great expense) in the real world, and could either be internal (based on endogenous characteristics of the system) or external (resulting from exogenous effects). However, by manipulating both the decision factors and the noise factors during laboratory experiments, a statistical design-of-experiments approach could be used to systematically seek improved product designs.

In the parameter design (or *robust design*) stage, the analyst conducts a designed experiment to gather information about the expected system performance across the noise space. The ideal system configuration is one that results in a mean performance equal to the target τ , and a performance variability of zero. Since in practice the ideal is unattainable, a loss function serves to trade off average deviation from the target with consistency of the output. The “best” system is thus often not that associated with the best mean performance. For example, Quinlan (1985) described how a redesigned speedometer cable resulted in an over ten-fold savings in expected warranty claims because of reductions in the mean and variance of cable shrinkage. Sanchez et al. (1998) examine a job shop where loss is a function of the time jobs are in the system. They found the optimal shop floor layout and control resulted in over 35% savings when compared to the configuration yielding the lowest mean. Risk and performance trade-offs are routinely considered in other fields, such as financial portfolio management, although they have not yet benefitted from the formal application of the robust design approach.

The final stage in Taguchi’s framework is called *tolerance design* (Taguchi, 1986, 1987; see also D’Errico & Zaino, 1988.) At this stage, the levels for the decision factors have already been chosen to achieve a good product design. The analyst conducts a further statistical experiment to evaluate the overall system performance and attribute variation in the response to variation in the noise factors. Any decision factors that cannot be precisely controlled in the manufacturing environment, but are randomly distributed about their chosen values, are also considered sources of noise. By incorporating the loss function, the tolerance design results can suggest several ways for further improving the product design. They indicate whether or not upgrades in the consistency of component parts are cost-effective, or whether any specifications could be relaxed without adversely affecting product quality. In addition, by quantifying the impact of the noise factors on the expected loss, they highlight which (if any) sources of noise should be targeted for improvement in the future.

In this paper, we focus on using designed experiments to evaluate the life cycle cost of a particular system, where the noise factors represent uncertainties in future component costs. In manufacturing applications, tolerance design experiments are typically set up to detect only main effects, either using Taguchi’s orthogonal arrays or other classic orthogonal designs. Analysts have, by construction, guaranteed that the noise factor settings are uncorrelated during the experiment. However, it is still possible for some of these factors to be correlated—perhaps strongly—in the real world setting under normal operating conditions. If so, this raises several questions: What effect does correlation have on the tolerance design results? How can data obtained from an orthogonal experiment be used for



noise factor assessment when two or more of these factors are correlated? Are there better alternatives for the experimental design if correlation is known to exist *a priori*?

Our goal in this paper is to show that it is possible to construct robust cost or performance estimates for situations where strong pairwise correlations are present among the noise factors. We motivate the need for robust cost estimation using an example of current interest to the Marine Corps Expeditionary Energy Office. We then review a response-surface modeling approach for tolerance design (Vining & Myers, 1990; Myers et al., 1991; Ramberg et al., 1991), describe modifications in the analysis to account for such correlation, and present a class of elliptical designs that can be used when orthogonal designs over the entire range of interest are inappropriate.

Motivating Example: Marine Corps Expeditionary Energy

Our motivating example is drawn from Morse (2014), who explores in great detail the performance of a model that can be used to predict the energy needs for Marine Corps expeditionary operations. In this paper, we consider a single use-case from Morse's study to illustrate the need for robust cost estimates, as well as how appropriate experimental designs can be used to provide more insight to program managers and planners about the projected operational cost/benefit of investments in alternative energy.

Marine Corps Expeditionary Energy Initiatives

General Amos published the Marine Corps Expeditionary Energy Strategy on March 21, 2011. This energy strategy sets an objective of making 50% of Marine Corps bases "net-zero energy consumers" by 2020 (ALMAR011/11, 2011). In 2011, fuel consumption in Afghanistan was estimated at 8 gallons per Marine per day (Hersterman, 2011). In the Expeditionary Energy Strategy, General Amos focused on the deployed environment and called for a 50% reduction in fuel consumption per Marine down to 4 gallons per Marine per day (Amos, n.d.). The Marine Corps' reduction in fuel consumption will result not only in increased maneuverability and sustainability, but also in reduced fuel-supply related casualties.

To accomplish this reduction in fuel consumption, the Marine Corps first focused on reducing the fuel consumption of forward operating bases (FOB). The Marine Energy Assessment team identified that 32% of fuel consumed by the Marine Expeditionary Brigade (MEB) deployed to Afghanistan in 2009 was used for electric power generation (Schwartz, Blakeley, & O'Rourke, 2012).

Through the efforts of the Expeditionary Energy Office, the Office of Naval Research (ONR), and their interaction with industry, the Marine Corps has developed robust, renewable technologies to meet the energy objectives laid out in the Commandant's energy strategy. Through the EEO the Marine Corps has investigated energy solutions in such areas as photovoltaic arrays for power harvesting, light emitting diodes (LED) for decreased energy consumption, and improved battery and smart power controller technologies for better energy management.

Two successful renewable energy assets developed by the Marine Corps are the Ground Renewable Expeditionary Energy System (GREENS) and the Solar Portable Alternative Communications Energy System (SPACES). GREENS is a power generation and conversion system that allows Marines to power systems with solar energy. Each GREENS is comprised of eight photovoltaic array panels, four high-energy lithium batteries (HELB), and a central controller. Figure 1 shows how all components of a GREENS are combined to harvest solar power, receive AC and DC power, employ the HELB batteries, and to provide DC output for a load.



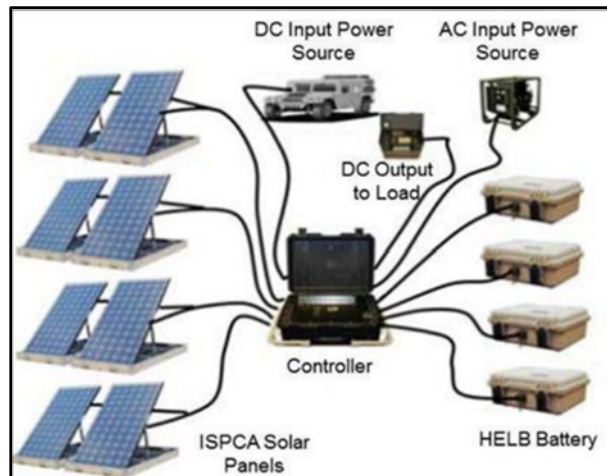


Figure 1. GREENS Employed With All Photovoltaic Arrays and High Energy Lithium Batteries
(USMC Warfighting Laboratory, 2012)

The SPACES system is much smaller, lighter, and less powerful than GREENS. Powered by two (12) volt folding portable solar panels, a single SPACES is designed to recharge two BB-2590 lithium batteries or power battery operated devices such as laptops or radios; SPACES can also be powered from batteries or running vehicles if solar power is unavailable (USMC Warfighting Laboratory, 2012).

While a single GREENS can provide 300 watts of power for 24 hours, GREENS systems are modular and can be combined into as large as a five GREENS system, providing for peak power requirements of up to 1000 Watts (1kW). The GREENS' modular design also allows the user to employ fewer than the full 8 solar panels and fewer than the full four HELB batteries if desired, to configure the GREENS to meet smaller load requirements. The first GREENS unit was tested in July 2009. The CMC approved accelerated fielding of GREENS and SPACES in April 2011, and fielding began in early 2012 (USMC Center for Lessons Learned, 2012).

There are two general approaches for employing renewable energy technologies to reduce fuel consumption. The first approach decreases the peak levels of a load by removing components of that load and powering them separately with renewable energy technology such as PV arrays, batteries, and wind turbines. To ensure reliable availability of power, this will usually also include using a conventional generator as a backup to supply power in times of poor weather. The Marine Corps currently employs the GREENS in this way. The second approach employs the renewable energy technologies to decrease the operating time of any AC generator(s) covering the load. This combines the generator and renewable energy source into a hybrid system that passes the load between renewable power sources and diesel generators depending on load size and renewable power production. In many situations, this method of employing a renewable energy technology can do more to decrease fuel consumption and allow for higher generator operating efficiency than the first technique described. The Marine Corps began its pursuit of hybrid systems capable of powering 3kW to 300kW micro-grids (USMC Expeditionary Energy Office, 2013). In this paper, we focus on using GREENS in off-the-grid capacities.

Equipment	Average Hourly Power Required (W)	Peak Power Required (W)
GBOSS Heavy (w/2 40" LCDs)	961	800
VRC-110 w/Blue Force Tracker	165	440
PRC-150	57	375
Coffee Pot	45	975

Figure 2. Examples of Common Marine Corps Equipment the GREENS System Can Power, With Associated Power Requirements
(USMC Warfighting Laboratory, 2012)

The Hybrid Optimization of Multiple Energy Resources (HOMER)

Beyond the renewable technologies and hybrid systems themselves, another tool the Marine Corps has pursued as part of its energy strategy is the Hybrid Optimization of Multiple Energy Resources (HOMER) model (HOMER energy, n.d.). HOMER is a deterministic, time-step model of micropower systems. It can model both conventional systems such as diesel-powered generators, and renewable power sources such as photovoltaic arrays and wind turbines. The HOMER model has been utilized for years by organizations and companies across the globe, to assist them in their cost effective employment of renewable energy sources and appropriately sized generators for the long term powering of facilities. There is potential for HOMER to serve as a useful Marine Corps Modeling and Simulation tool for planning efficient and effective expeditionary micropower systems, by helping Marine Corps power planners and logisticians anticipate the fuel consumption savings to be gleaned from employing hybrid systems to support a given load requirement for a particular location and time frame. To be useful for modeling expeditionary microgrids, HOMER must be robust across a wide range of locations, microgrids, compositions, and load profiles.

The U.S. National Renewable Energy Laboratory (NREL) developed HOMER in 1993 as a part of its Village Power Program. The model was designed to assist users in designing micropower systems and modeling their performance under specific conditions. Although originally built only for consideration of off-the-grid micropower systems, the model was updated in 2000 to accommodate the modeling of grid-tied systems as well. The HOMER application simulates and measures the performance of each power generation asset available, both individually and in hybrid configurations. In this way, the model is used to identify the most cost-efficient micropower system design for meeting long term electric load requirements.

In order for the HOMER model to simulate the performance of the solar panels, the user must load the solar resource and temperature profile into the model. For years, the solar industry has relied upon NREL's Typical Meteorological Year (TMY) data set for modeling the performance of solar power systems (Williams & Kerrigan, 2012). A TMY is a statistically derived profile of a typical meteorological year for certain locations across the United States. NREL's TMY data consists of hourly measurements of solar irradiance and certain meteorological elements and has been updated three times since its establishment in 1978 by Sandia National Laboratories (Wilcox & William, 2008). The current TMY, TMY3, was created with measurements acquired from 1976 to 2005. TMY3 data can be imported into HOMER for given localities.



Previous HOMER Assessment

Marine Corps expeditionary operations involve relatively small units conducting fast paced and short duration operations. The units depend on robust, space efficient, and weight efficient sources of power. Logistics planners and commanders must be able to rely on their energy source, and variability in solar irradiance is one element that brings that reliability into question. Solar irradiance variance can be caused by multiple factors, including varying cloud cover and pollution.

In 2010, Major Brandon Newell conducted an experiment where he assessed the capabilities of the HOMER model in forecasting the power output of a solar panel at the Naval Postgraduate School (Newell, 2010). This initial research found that, when employing monthly temperatures averages and synthetic solar irradiance profiles built using the algorithm of Graham & Hollands (1990) for model inputs, the HOMER model performed with an unacceptable degree of fidelity, with HOMER estimating “an energy production level that was over 25% higher than the actual measured energy” (Newell, 2010). Major Newell attributed this overestimate of power production to three factors: a disparity between measured and anticipated surface solar irradiance, a disparity between measured and anticipated ambient temperature, and an underestimate of the de-rating value for the solar panels.

Major Newell’s 2010 thesis research demonstrated that solar irradiance variance from the anticipated values will result in inaccurate power production predictions by the HOMER model. He also demonstrated that the percentage of solar irradiance disparity does not account for the percentage of inaccuracy created in predicted power output. While the anticipated solar irradiance profile overestimated actual solar irradiance by 9.35%, this did not equate to the model overestimating PV power production by 9.35%—instead, the HOMER model overestimated the PV power production by 27%. As Newell (2010) pointed out, this is “due to the nature of the comparison, which only compared the total kW per m squared for the month and disregarded when the disparities occurred.” The amount of solar irradiance variability that occurs for a given scenario does not necessarily equate to an equivalent amount of PV power production variability, but there is a direct relationship between solar irradiance and PV production variability that must be identified.

The 27% overestimate in energy production, identified in Newell’s thesis work, was predicted using solar irradiance and temperature profiles. Solar irradiance profiles created using average monthly solar irradiance values acquired from NASA Surface Solar Energy Data Set and employment of the Graham-Hollands algorithm to create synthetic profile based on the average monthly solar irradiance values. Temperature profiles consisted of monthly temperature averages for the location. To identify the impact of discrepancies between the anticipated and real temperature and solar irradiance profiles, Major Newell reran the model with the measured temperature and solar irradiance profiles for that period of time. The results of these new HOMER runs showed that the differences between real world and anticipated temperature and solar irradiance profiles accounted for a 10% overestimate: a 6% overestimate in power production was due to differences between real and anticipated temperature profiles, while a 4% overestimate in PV power production was due to differences between real and anticipated solar irradiance profiles (Newell 2010). This still leaves a large gap between the predicted and actual performance of the PV arrays.

Assessing the Robustness of the HOMER Model

HOMER is designed to identify the most fuel-efficient (i.e., cost-effective) solution for a given load profile at a fixed location, as described above. The answer is a single “optimal”



configuration, and a specified fuel usage/overall cost. We now examine several extensions that seek to reveal the robustness of this type of solution.

Exploring Spatial Variability

The nature of Marine Corps expeditionary operations makes the effects of irradiance variance even more important than in the commercial settings of the solar industry. Due to the unpredictable nature of combat and humanitarian operations, the Marine Corps does not have the luxury of being able to gather data on the solar radiance and weather patterns of a location for months (or years) prior to deployment. Figure 3 shows how the TMY3 data varies by location in the United States. Clearly, the location plays a vital role in determining the utility of PV arrays. Microclimates also have an effect. For example, arrays set up near tall trees, tall buildings, or a steep hillside produce noticeably less power than arrays set up a short distance away without obstructions.

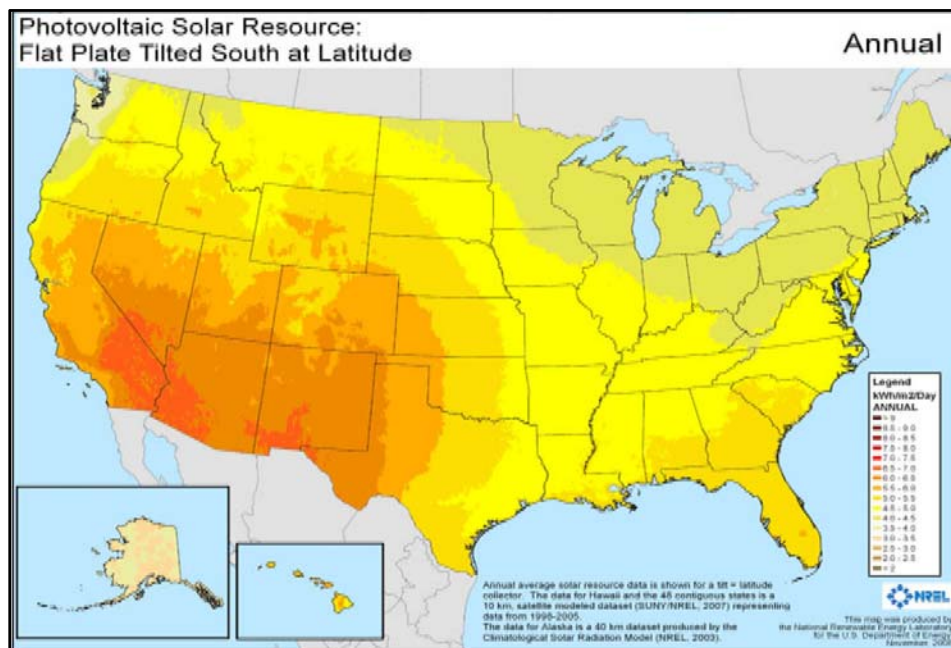


Figure 3. Annual Solar Irradiance in the United States
(USEIA, 2013)

For purposes of illustration, we restrict our investigation to 60-day operations taking place in Salt Lake City, UT, beginning on the 75th day of the year. For a much broader investigation of 10 U.S. cities, other operation start times, and other operation duration times, see Morse (2014). To be useful for deployment to unanticipated locations, HOMER must be robust enough to handle the solar irradiance and temperature variances of those locations. Profiles for generic regions (desert, jungle, mountain, etc.) are desirable. Such profiles will be associated with greater uncertainty than those for a known location, but are beyond the scope of this paper.

Exploring Temporal Variability

The shorter term duration of expeditionary operations means that PV systems used by the Marine Corps are also quite susceptible to the effects of temporal solar irradiance variability. This is not surprising: TMY3 data is intended for use in simulating solar power systems over “a longer period of time, such as 30 years” (Wilcox and William, 2008). In fact, the first page of the TMY3 User Manual warns in italics: “The TMY should not be used to

predict weather for a particular period of time” (Wilcox & William, 2008). The subplots in Figure 4 make this temporal variation apparent on a monthly basis, but still portray only a portion of the true variability.

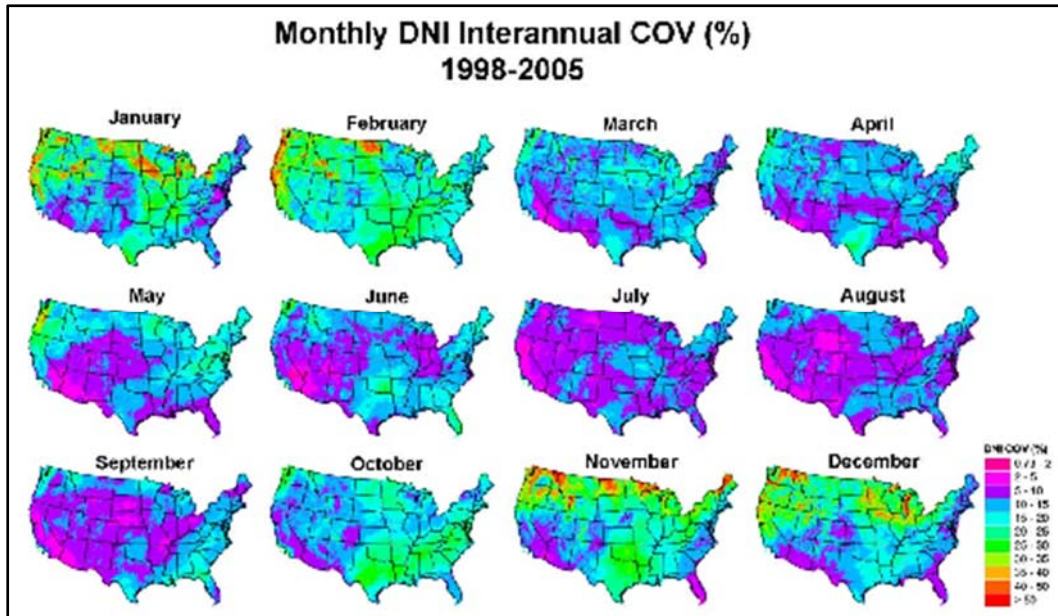


Figure 4. Monthly Direct Normal Irradiance (DNI) Interannual Coefficient of Variation (COV) in the United States
(Gueymard & Wilcox, 2011)

As an example, consider two graphs that show the variability in 60 days of solar irradiation for Salt Lake City (Figures 5 and 6), beginning on the 75th day of the year. The first indicates that although the TMY average is 317 kilowatt-hours per square meter (kWh/m²), it ranges from a low of 263 kWh/m² to a high of 359 kWh/m²: the coefficient of variation (σ / μ) is 7.14%.

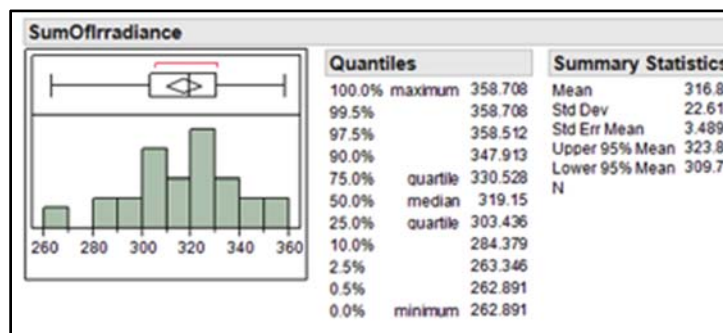


Figure 5. Histogram of Total Solar Irradiation Over Days 75–134 for Salt Lake City, by Year, 1961–2010

A closer look at the data reveals much more. Figure 6 plots the annual solar irradiation by year. The line represents the least-squares regression trend, the dark pink region represents a 95% confidence interval for the mean response, and the light pink region represents a 95% prediction interval for an individual year’s response. The trend is statistically significant (p-value < 0.0001).

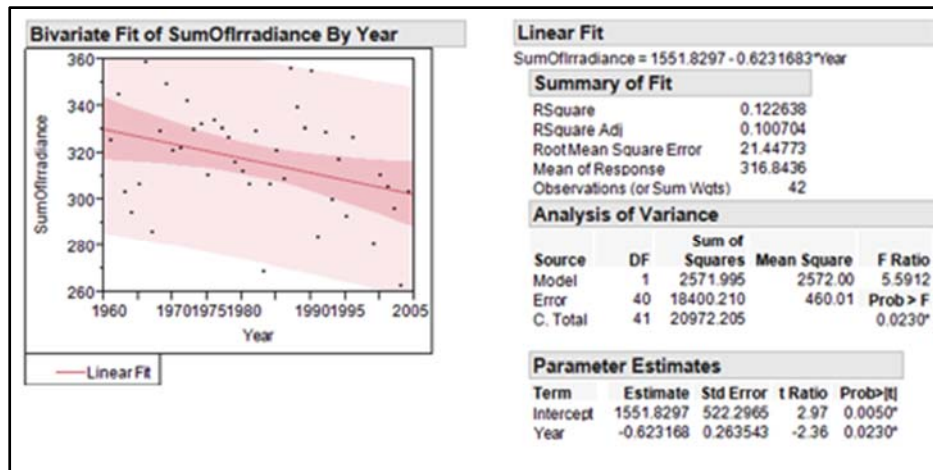


Figure 6. Scatterplot of Total Solar Irradiation Over Days 75–134 for Salt Lake City, by Year, 1961–2010

Morse (2014) found similar patterns for the other nine cities he studied. After further inquiry, he found this trend was a manifestation of a phenomenon known as “global dimming” (Muller, 2014). Global dimming is described as the “decadal decrease of surface solar radiation” (Wild, 2009). The name “global dimming” was coined by Stanhill & Cohen in their 2001 article “Global Dimming: A Review of the Evidence for a Widespread and Significant Reduction in Global Radiation” (Stanhill & Cohen, 2001). The “global” portion of the name does not refer to the phenomenon having a universal effect across the world but instead refers to “the sum of diffuse and direct solar radiation,” that is to say global radiation (Wild, 2009). The dimming refers to a decrease in that global radiation which was measured as occurring at different rates across the world. In the 1980s and 90s climate modelers began to distinguish a trend of decreasing surface solar radiation in available surface solar radiation records dating back to the 1950s. The rates of the decrease differed by location but were mostly seen as occurring from the 1950s up to the 1980s Muller, 2014). Later studies, focusing on the period from the 1980s to 2000s, identified an apparent shift in the trend to a possible increase in solar irradiance. This trend was named “global brightening.”

The performance of the model with regard to long-term solar irradiance trends is important because of its effect on each solar power system’s performance over its life cycle. GREENS performance estimates based off of ten-year-old TMY data, for example, will overestimate the solar irradiance available to power the system where there is a negative linear relationship between time and solar irradiance. Morse (2014) provides a more detailed discussion of the global dimming effects as they relate to the use of HOMER.

Exploring the Impact of Correlated Costs

We have already discussed several of the inputs to the HOMER model, including the resources available (e.g., generators, PV arrays), the location and associated solar and temperature information (either as typical years, or actual data), load profile requirements, operational duration, and operational start. Other inputs that we have not yet discussed include cost information—specifically, costs of capital, replacement, fuel, and operations and maintenance (O&M) costs of power components (generators, PV arrays, wind turbines, and others modeled by HOMER). The user specifies these costs before HOMER is executed. Once all this information is set, then HOMER will output the configuration it deems “optimal” for the specific deterministic setting, and provide as deterministic outputs the expected costs

and energy usage associated with each platform. Presumably, this is the system configuration that will be chosen for that type of operation.

The default inputs for HOMER assume that the relative costs of conventional fuel and alternative energy sources remain constant. However, this is unlikely to hold. For example, one could argue that as non-renewable energy sources are depleted and become scarcer, they will become more expensive—and that the costs for renewable energy generators will tend to be higher as well, because of competing demands for limited resources. If so, this assumes there will be a positive correlation between the two types of costs in the future. Alternatively, one could argue that high costs for non-renewable sources will result in additional R&D efforts put toward renewable energy platforms, so there will be a tendency for these two costs to be negatively correlated in the future. Indeed, such projections are already available. For example, Figure 7(a) (U.S. Energy Information Administration, 2014) shows three variants of oil cost projections over the next 25 years: a reference line, as well as low and high oil price projections. Figure 7(b) (adapted from U.S. Department of Energy, 2014) shows a single cost projection for PV arrays over a different time frame. We see that if the low oil price projection holds, the two energy costs will be positively correlated over the 2014-2020 time frame. In the other two circumstances, the two energy costs will be negatively correlated.

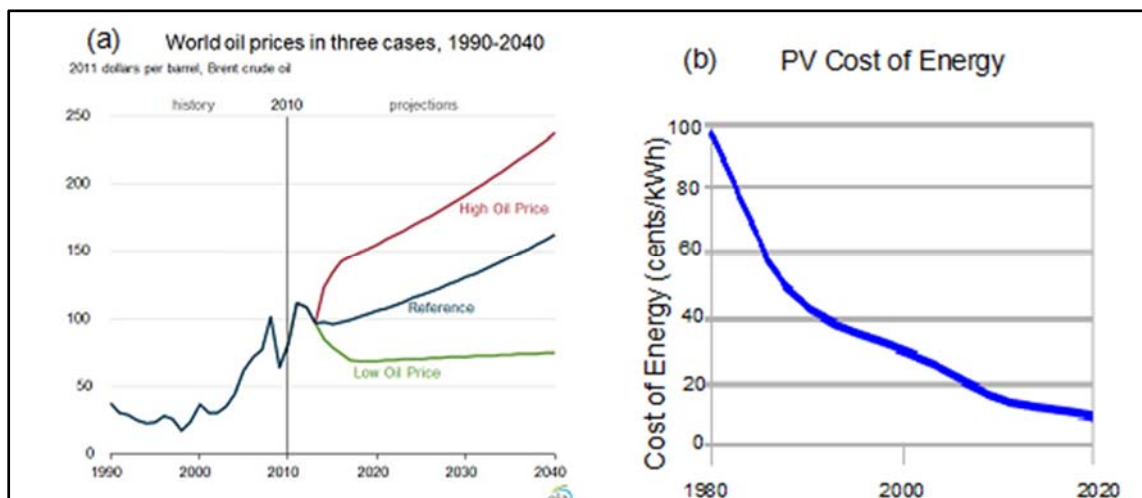


Figure 7. Oil Cost Projections and PV Array Cost Projections
 ([a] USEIA, 2014; [b] adapted from USDOE, 2014)

What is the potential impact of this source of uncertainty on the life cycle cost outputs from the HOMER model? To answer this question, we will leverage the field of design of experiments (DOE) in order to quickly calculate the results. However, the standard DOE approaches are not suitable in the presence of correlation. We provide technical justification in the next section, and then return to our example.

Methodological Development: Designs for Correlated Noise Factors

Let Y denote the performance measure of interest, W_1, \dots, W_k denote the noise factors controlled during the course of the experiment, and let μ_i and σ_i denote the mean and standard deviation of W_i ($i = 1, \dots, k$). Then, assuming that the noise factor ranges are small enough that a linear model is appropriate, we have

$$Y = \beta_0 + \beta_1 W_1 + \beta_2 W_2 + \dots + \beta_k W_k. \tag{1}$$

An orthogonal experimental design (often a factorial or fractional factorial) is used for collecting data regarding the process. Under an independence assumption, setting the levels for noise factor W_i at $\mu_i \pm \sigma_i$ will result in a two-point distribution with the same mean and standard deviation as the underlying distribution. After data are gathered, a linear model is fit:

$$\hat{Y} = \hat{\beta}_0 + \hat{\beta}_1 W_1 + \hat{\beta}_2 W_2 + \dots + \hat{\beta}_k W_k \quad (2)$$

Assuming that the W_i are independent and normally distributed, then the model of Equation 2 can be used to determine the overall system mean and variance by treating the estimated coefficients as constants:

$$\mu_Y \approx \hat{\beta}_0 + \hat{\beta}_1 \mu_1 + \hat{\beta}_2 \mu_2 + \dots + \hat{\beta}_k \mu_k \quad (3)$$

$$\sigma_Y^2 \approx \hat{\beta}_1^2 \sigma_1^2 + \hat{\beta}_2^2 \sigma_2^2 + \dots + \hat{\beta}_k^2 \sigma_k^2 \quad (4)$$

From Equation 4, we can estimate a transmitted variance for each noise factor i , which is the variability in the response that is attributable to W_i :

$$\sigma_{t;i}^2 \equiv \hat{\beta}_i^2 \sigma_i^2. \quad (5)$$

The dependence of $\sigma_{t;i}$ on the regression coefficient means that it is possible for a particular noise factor's variance to be magnified or dampened as it is transmitted through to the response. The ratio $(\sigma_{t;i} / \sigma_Y)^2$ is the proportion of the variability in the response that is attributable to W_i . Potential changes to the noise factors, that affect only the variance, not the mean, can then be evaluated by considering the reduction on the overall performance variability σ_Y^2 and the corresponding reduction in cost.

Now suppose that two of the k noise factors (W_1 and W_2) have a correlation of ρ in the real world, and all other noise factor pairs are independent. In this case, the value of μ_Y remains unchanged from that computed in Equation 3. However, the overall variance now is

$$\sigma_Y^2 \approx \hat{\beta}_1^2 \sigma_1^2 + \hat{\beta}_2^2 \sigma_2^2 + 2\rho \hat{\beta}_1 \hat{\beta}_2 \sigma_1 \sigma_2 + \hat{\beta}_3^2 \sigma_3^2 + \dots + \hat{\beta}_k^2 \sigma_k^2 \quad (6)$$

which is greater than the value in Equation 4 if $\rho > 0$ and less than this value if $\rho < 0$. This means that the overall estimate of system variability and the transmitted variance proportions are different than those calculated assuming independence.

If the W_i ($i = 1, \dots, k$) are truly independent, the transmitted variances completely separate the effects for the various noise factors. This does not occur when W_1 and W_2 are correlated, although orthogonal experimental designs might be desirable because of the increased precision of the estimated coefficients. However, the results are no longer separable in the real world. Rather than compute individual transmitted variances for each of the two factors, we use a joint transmitted variance:

$$\sigma_{t;1,2}^2 = \hat{\beta}_1^2 \sigma_1^2 + \hat{\beta}_2^2 \sigma_2^2 + 2\rho \hat{\beta}_1 \hat{\beta}_2 \sigma_1 \sigma_2 \quad (7)$$

Potential changes to the system components can then be assessed by determining the resulting changes in the joint transmitted variance and the overall system variance.

This approach can be generalized in a straightforward manner to situations where multiple pairs of correlated noise factors exist. As above, we construct linear models for the mean and variance of the performance measure Y as functions of the noise factors W_i ($i = 1, \dots, k$):



$$Y \approx \hat{\beta}_0 + \sum_{i=1}^k \hat{\beta}_i W_i. \quad (8)$$

Treating the regression coefficients in Equation 8 as constants, we obtain

$$\sigma_Y^2 \approx \sum_{i=1}^k \hat{\beta}_i^2 \sigma_i^2 + 2 \sum_{i=1}^k \sum_{j=i+1}^k \rho_{i,j} \hat{\beta}_i \hat{\beta}_j \sigma_i \sigma_j \quad (9)$$

where ρ_{ij} denotes the correlation between W_i and W_j . Joint transmitted variances can be computed as in Equation 7.

In some situations, the correlation in the real world may restrict the choice of the design: a factorial or fractional factorial design covering the entire range of interest may be impossible to conduct. For example, a queueing system might be unstable if all noise factors are held at their high levels. If this situation were unlikely to occur in practice because of negative correlation among the variables, then a sampling scheme that makes use of the underlying dependence structure would seem more appropriate. Alternatively, it may be that the statistical response-surface models are developed from observational rather than experimental data. Although such models can be analyzed *post hoc* by conducting orthogonal experiments involving the noise factor settings, this approach is questionable if the model was not constructed using similar combinations. Large extrapolations of the fitted model might not be at all close to the true response surface. In addition, if certain combinations of the factors are not likely to occur in practice, then we lose the benefit of sampling at levels such as $\mu \pm \sigma$ in order to achieve the same variability in the sampling distribution as in the underlying normal distribution.

Once again, for simplicity, we assume that the noise factors are normally distributed but only the first two (W_1 and W_2) are correlated. We also assume, without loss of generality, that $\mu_i = 0$ and $\sigma_i = 1$ ($i = 1, \dots, k$). This corresponds to standardizing each of the noise factors by subtracting its mean and dividing by its standard deviation before conducting the experiment. The joint distribution of W_1 and W_2 is then a bivariate normal. Letting W_1 be on the x-axis and W_2 on the y-axis, the contours of the bivariate distribution are elliptical, satisfying

$$x^2 - 2\rho xy + y^2 = r^2 \quad (10)$$

as long as $|\rho| < 1$ (Dudewicz & Mishra, 1987).

If $\rho = 0$, then Equation 10 reduces to a circle with radius r centered about the origin. If $\rho > 0$, then the major axis of the ellipse falls on the line $y = x$ and the minor axis is along the line $y = -x$, as shown in Figure 8. If we ran our experiment as if W_1 and W_2 were independent, then a 2-level factorial would result in sampling at the 4 points $(\pm 1, \pm 1)$. These correspond to sampling each of the two factors at $\mu_i \pm \sigma_i$, so that the discrete sampling distributions for W_1 and W_2 have the same mean and variance as the marginal distributions. An alternative, which looks much more reasonable in the presence of correlation, is to sample at points on one of the elliptical contours.

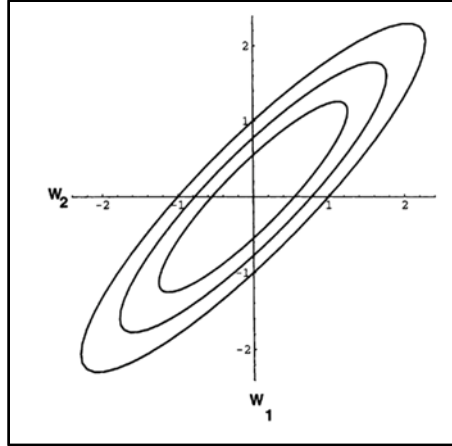


Figure 8. Density Contours for a Bivariate Standard Normal With Correlation Coefficient $\rho = 0.9$

From Equation 10 and basic geometry (Beyer, 1987) one can compute coordinates of the major and minor axial points for given r . Equations 11 and 12 hold when $\rho > 0$, when standardized units are used for both noise factor designs. If $\rho < 0$ then Equation 11 gives the minor axial points and Equation 12 gives the major axial points.

Major Axial Points

$$\pm \left(\frac{r}{\sqrt{2(1-\rho)}}, \frac{r}{\sqrt{2(1-\rho)}} \right) \quad (11)$$

Minor Axial Points

$$\pm \left(\frac{-r}{\sqrt{2(1+\rho)}}, \frac{-r}{\sqrt{2(1+\rho)}} \right) \quad (12)$$

If we sample at the four axial points, then the variance of the sampling distribution for either W_1 or W_2 will be

$$\begin{aligned} \sigma_W^2 &= \frac{1}{4} \left(\frac{r^2}{(1-\rho)} + \frac{r^2}{(1+\rho)} \right) \quad (13) \\ &= \frac{r^2}{4} \left(\frac{1+\rho+1-\rho}{(1+\rho)(1-\rho)} \right) = \frac{r^2}{2(1-\rho^2)} \end{aligned}$$

In order to achieve appropriate marginal variances, set Equation 13 equal to the marginal variance ($\sigma_1^2 = \sigma_2^2 = 1$) and solve for r . This yields $r^2 = 2(1-\rho^2)$, so the experimental design will consist of sampling at the major and minor axial points of the ellipse specified by

$$x^2 - 2\rho xy + y^2 = 2(1 - \rho^2) \quad (14)$$

A plot of such ellipses is shown in Figure 9, with correlations ranging from zero (a circle) to 0.9. For negative correlations, the mirror image of this figure is appropriate. The standard two-level factorial design (with sampling of both factors at one standard deviation below and one standard deviation above the mean) is the limiting case as ρ approaches zero. However, the design is quite different if correlation is present: the individual factor ranges are larger than $\mu_i \pm \sigma_i$, but the two-dimensional region over which sampling takes place is narrower.

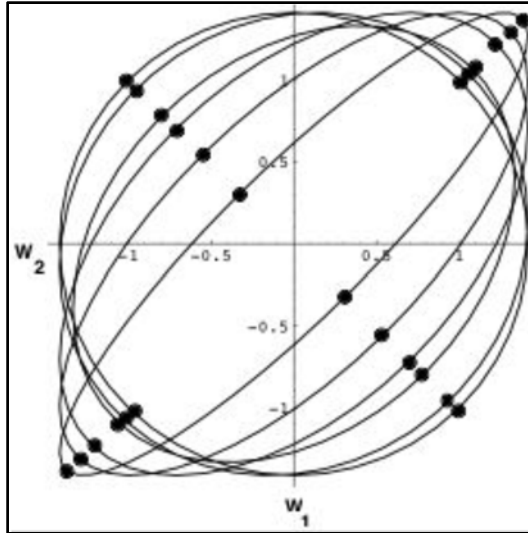


Figure 9. Elliptical Design Points for Two-Level Sampling Under Correlation, for $\rho = 0$ (Circle), 0.1, 0.3, 0.5, 0.7, and 0.9

These elliptical designs were introduced in Sanchez (1994b), where they were illustrated for two diverse applications: a deterministic circuit model, and a stochastic home mortgage portfolio model.

For a deterministic model, such as the HOMER example used in this paper, the transmitted variances for the noise factors sum to the overall system variance. In discrete-event simulation experiments, this is generally not the case: although many noise factors can be explicitly controlled, the system is characterized by some inherent variability that remains unexplained by any noise factors. Tolerance design analysis must therefore be modified to take this into account (Sanchez, 1994a; Sanchez et al., 1998). In order to reflect the true system variability, the overall system variance estimate of Equation 4 is augmented by incorporating estimates of the system variability obtained within simulation runs. This augmented analysis should be used for either orthogonal or elliptical tolerance experiment designs so the results reflect the true system variability.

Correlated Costs for the HOMER Example

We now illustrate the approaches for the HOMER example. We simplify the setting for illustration purposes. Our assumptions follow.

- Let F denote the number of liters of diesel fuel used.
- We are concerned with two noise factors: W_d is the cost of diesel fuel (\$/liter), and W_{pv} is the purchase cost of PV arrays (\$/kW peak load requirement). We assume that these noise factors are normally distributed: $W_d \sim N(1, 0.37^2)$ and $W_{\{pv\}} \sim N(360, 66.6^2)$.
- Our peak load requirement for the 5 GREENS system is 1 kW, and the liters of fuel used are determined from HOMER.
- We remove the linear global dimming trend from the data, and treat the variation around this trend line (due to variation in solar irradiation and temperature) as the intrinsic variability in the system.
- Our response Y is computed by considering the peak requirement for the 5 GREENS system ($n_{pv} = 5$) and the liters of diesel fuel saved (n_d):

$$Y = n_{pv}W_{pv} + FW_d.$$

This is the energy cost if the PV arrays are used for a single operation. A more realistic assumption is that they will be used for multiple operations, in which case the cost of the arrays would be prorated accordingly. In our simple example, we use Y to compare the relative merits of different alternatives.

- We ignore all other costs and discount factors.

Consider three different correlations for the noise factors W_d and W_{pv} : $\rho = 0$ (no correlation), $\rho = 0.9$ (strong positive correlation), and $\rho = -0.9$ (strong negative correlation). Figure 10 illustrates the differences between several of the estimates that we have discussed. In Figure 10(a) we plot (i) the deterministic answer from HOMER, using TMY inputs for both solar and temperature, and the expected noise factor costs; (ii) the distribution one might use based on the recorded solar irradiation and temperature variability if one assumed the data from different years were independent and identically distributed; and (iii) the predicted distribution based on the different solar irradiation and temperature variability—this removes the global dimming trend, and represents the intrinsic variability in the system (at least for short-term projections). This clearly illustrates the importance of exploring the uncertainty in the potential operational environmental conditions, in order to convey the resulting risk to the decision maker. For example, while Marine Corps officers might not be interested in estimating cost when planning an expeditionary operation, the amount of conventional fuel saved might directly affect the length of time they can sustain this operation before resupply.

In Figure 10(b) we include uncertainties in the noise factors (future PV array cost and diesel fuel cost) to the one-year projection that incorporates global dimming. Note the vastly different scales in Figures 10(a) and 10(b). This shows how uncertainties in future costs—and the correlations in these uncertainties—translate to probabilities of cost overruns. This may be of interest to program managers as they seek to acquire new systems. In our example, all three of the correlation assumptions yield distributions with the same mean (\$5,189), but the standard deviations (σ 's) differ. The smallest σ occurs when the future costs of PV arrays and diesel fuel are negatively correlated, and the largest σ occurs when they are positively correlated.



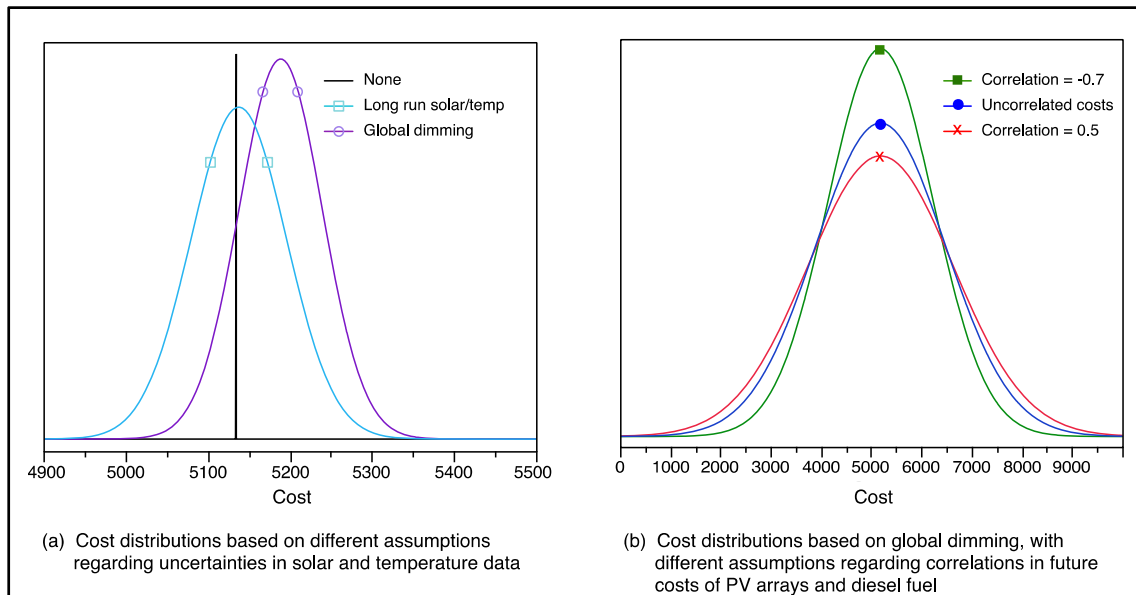


Figure 10. Distributions of Y (Combined Cost) Based on Different Assumptions for Uncertainties in Future Solar, Temperature, and Cost Component Distributions

The different distributions translate to different risks of exceeding particular cost thresholds. Numerical comparisons are easier to show using cumulative distribution plots, as in Figure 11, instead of the density plots in Figure 10(b). Figure 11 shows that a program manager interested in estimating the probability of exceeding a cost threshold of \$7,000 can use the appropriate curve. This probability is 0.894 (89.4%) when $\rho = 0.5$, 0.918 when $\rho = 0$, and 0.958 when $\rho = -0.7$. (Alternatively, if one were interested in the cost threshold that would be exceeded with probability at most 0.10, this translates to cutoffs of \$7,047, \$6,833, and \$6,533, for $\rho = 0.5, 0$, and -0.7 , respectively. In some instances, differences in risk might be enough to change a decision to continue with a program, and care should be taken to select appropriate noise factor distributions and correlations. In our example, the striking differences between estimates in Figures 10(a) and 10(b) indicate that including the noise factor distributions at even a rough level is extremely informative. Ignoring these (Figure 10[a]) would lead a program manager to assume there was essentially no risk of cost exceeding \$5,400, when Figure 10(b) and Figure 11 show that the real risks would be over 44%.

These simple numerical examples are for illustration purposes only. To truly be useful for program managers, life cycle cost estimates (rather than one-year-out projections)—and a more comprehensive examination of the breadth of operational requirements and operational environments—are necessary. Furthermore, robust design principles can be used to seek system configurations that are robust to uncertainties in the environment, which is an important consideration for equipping expeditionary units. Once again, we refer the reader to Morse (2014), who conducted a much larger experiment over operations of start times, durations, and locations for units with different configurations of energy supply resources.

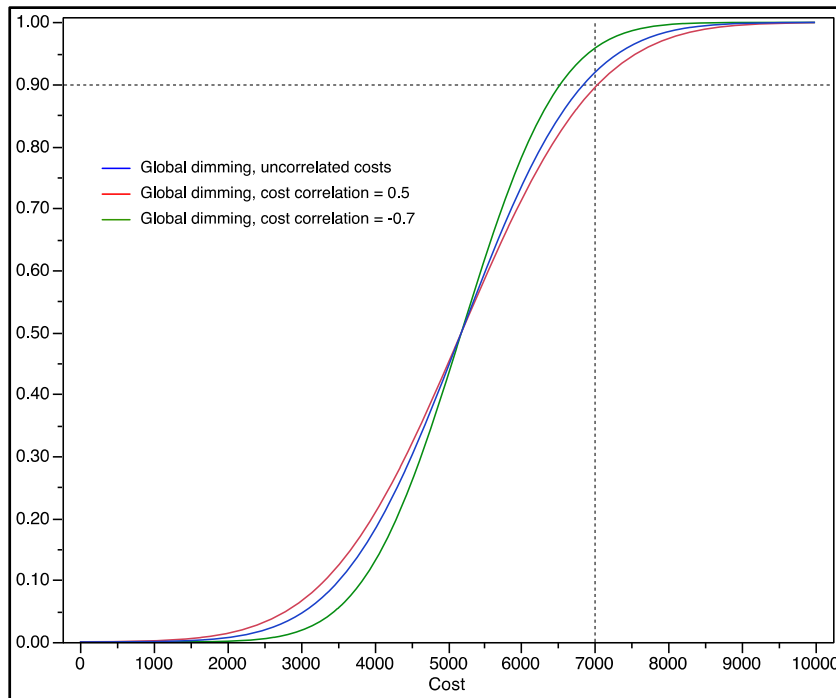


Figure 11. CDFs of Y (Combined Cost) Based on Different Assumptions for Cost Component Correlations, Using Global Dimming Results for Solar and Temperature Uncertainties

Concluding Remarks

In this paper, we provided motivation for the need to develop methods for conducting designed experiments involving correlated noise factors. We show how these can be used to obtain a more representative distribution of potential life cycle costs, so that program managers and planners can have better assessments of the potential risks associated with acquiring or employing particular systems. These robust assessments are important. By revealing the risk of budget overruns associated with going forward with a particular system, they provide the decision makers with much more information than a simple “yes or no” comparison to a fixed budget constraint. At the same time, a designed experiment approach can be much more efficient than Monte Carlo simulation. We are currently evaluating other types of space-filling designs that may be more suitable for situations where the uncertainties may be far from normally distributed.

From the applications perspective, this example in this paper is intended as a simple illustration of the need for robust cost estimation, rather than a definitive estimate for solar PV arrays. Other uncertainties in the environmental conditions, such as temperature variations, will also play a role. Many other components influence life cycle costs—O&M cost, cost of spare parts, and discount rates, to name a few. There are also intangibles that may be more difficult to quantify, but that play major roles in determining the value of these systems. For example, the ability to partially offset energy needs with PV arrays may increase the time an expeditionary unit conducting disaster relief efforts is self-sustainable: this, in turn, may influence its relief effort plans. Yet our preliminary work is promising. We hope the solar energy example in this paper motivates the need for obtaining robust cost estimates, and shows how robust design principles can assist in this estimation process.

References

- ALMAR011/11: Marine Corps expeditionary energy strategy. (2011, April). Retrieved from <http://www.marines.mil/News/Messages/MessagesDisplay/tabid/13286/Article/109473/marine-corps-expeditionary-energy-strategy.aspx>
- Amos, J. (n.d.). USMC expeditionary energy strategy. Retrieved from <http://www.hqmc.marines.mil/Portals/160/Docs/USMC%20Expeditionary%20Energy%20Strategy%20%20Implementation%20Planning%20Guidance.pdf>
- Beyer, W. H. (1987). *CRC standard mathematical tables* (28th ed.). Boca Raton, FL: CRC Press, Inc.
- D'Errico, J. R., & Zaino, N. A. (1988). Statistical tolerancing using a modification of Taguchi's method. *Technometrics* 30(1), 397-405.
- Dudewicz, E., & Mishra, S. (1988). *Modern mathematical statistics*. New York, NY: Wiley.
- Graham, V. A., & Hollands, K. G. T. (1990). A method to generate synthetic hourly solar radiation globally. *Solar Energy* 44(6), 333-341.
- Gueymard, C. A., & Wilcox, S. M. (2011). Assessment of spatial and temporal variability in the U.S. solar resource from radiometric measurements and predictions from models using ground-based or satellite data. *Solar Energy* 85(5), 1068-1084.
- Hesterman, D. (2011, March). Alternative energy on the frontlines. Retrieved from <http://scicom.ucsc.edu/publications/essays-profiles-pages/essay-hesterman.html>
- HOMER Energy (2014, March). Retrieved from <http://homerenergy.com>
- Morse, M. (2014). *An analysis of the HOMER energy micropower optimization model's robustness for Marine Corps expeditionary operations* (Master's thesis, Naval Postgraduate School). In process.
- Muller, B., Wild, M., Driesse, A., & Behrens, K. (2014). Rethinking solar resource assessments in the context of global dimming and brightening. *Solar Energy*, 99, 272-282.
- Myers, R. H., Khuri, A. I., & Vining, G. (1992). Response surface alternatives to the Taguchi robust parameter design approach. *The American Statistician* 46(2), 131-139.
- Newell, B. (2010). *The evaluation of HOMER as a Marine Corps expeditionary energy pre-deployment tool* (Master's thesis, Naval Postgraduate School). Retrieved from http://edocs.nps.edu/npspubs/scholarly/theses/2010/Sep/10Sep_Newell.pdf
- Quinlan, J. (1985). Product improvement by application of Taguchi methods. *American Supplier Institute News (special symposium edition)*, Romulus, MI, 11-16.
- Ramberg, J. S., Sanchez, S. M., Sanchez, P. J., & Hollick, L. W. (1991). Designing simulation experiments: Taguchi methods and response surface metamodels. *Proceedings of the 1994 Winter Simulation Conference*. Institute of Electrical and Electronic Engineers, Piscataway, NJ, 167-176.
- Sanchez, S. M. (1994a). A robust design tutorial. *Proceedings of the 1994 Winter Simulation Conference*. Institute of Electrical and Electronic Engineers, Piscataway, NJ, 106-113.
- Sanchez, S. M. (1994b). Experiment designs for system assessment and improvement when noise factors are correlated. *Proceedings of the 1994 Winter Simulation Conference*. Institute of Electrical and Electronic Engineers, Piscataway, NJ, 290-296.
- Sanchez, S. M., Sanchez, P. J., & Ramberg, J. S. (1998). A simulation framework for robust system design. In *Concurrent Design of Products, Manufacturing Processes and Systems*, Wang, B. (Ed). Gordon and Breach, Amsterdam, Netherlands, 279--314.
- Schwartz, M., Blakeley, K., & O'Rourke, R. (2012). *Department of Defense energy initiatives: background and issues for Congress* (CRS Report for Congress R42558). Washington, DC: Congressional Research Service.



- Stanhill, G., & Cohen, S. (2001). Global dimming: a review of the evidence for a widespread and significant reduction in global radiation with discussion of its probable causes and possible agricultural consequences. *Agricultural and Forest Meteorology*, 107(4), 255-278.
- Taguchi, G. (1986). *Introduction to quality engineering*, UNIPUB/Krauss International, White Plains, NY.
- Taguchi, G. (1987). *System of experimental design* (Vols. 1-2). UNIPUB/Krauss International, White Plains, NY.
- Taguchi, G., & Wu, Y. (1980). *Introduction to Off-Line Quality Control*. Central Japan Quality Association, Nagoya, Japan.
- United States Department of Energy, Energy Efficiency and Renewable Energy. (2014, March). Costs of Solar Power from Photovoltaics. Retrieved from U.S. DoE EERE website
http://www1.eere.energy.gov/tribalenergy/guide/costs_solar_photovoltaics.html
- United States Energy Information Administration (2013, July). International energy outlook 2013. Retrieved from U.S. EIA website
http://www.eia.gov/forecasts/ieo/liquid_fuels.cfm
- United States Marine Corps Center for Lessons Learned. (2012, December). Expeditionary energy in Afghanistan - unclassified/FOUO. Retrieved from
http://www.jhuapl.edu/ClimateAndEnergy/Presentations/2011/RT_6_Charette.pdf
- United States Marine Corps Expeditionary Energy Office. (2013). Brief to industry: mobile electric hybrid power sources (MEHPS) analysis of alternatives (AOA). Quantico, VA: Author
- United States Marine Corps Marine Corps Warfighting Laboratory. (2012). *Guide to employing renewable energy and energy efficiency technologies*. Quantico, VA: Author. Retrieved from <http://www.hqmc.marines.mil/Portals/160/Docs/X-File%20Guide%20to%20Renewable%20Energy%20and%20Energy%20Efficient%20Technologies%20Sep%2012.pdf>
- Vining, G. G., & Myers, R. H. (1990). Combining Taguchi and response surface philosophies:
A dual response approach. *Journal of Quality Technology* 22, 15-22.
- Wilcox, S. & William, M. (2008). *User's manual for TMY3 data sets*. Golden, CO: National Renewable Energy Laboratory
- Wild, M. (2009). Global dimming and brightening: A review. *Journal of Geophysical Research: Atmospheres* (1984-2012), 114, D00D16. doi:10.1029/2008JD011470
- Williams, M.K. & Kerrigan, S. L. (2012). How Typical is Solar Energy? A 6 year evaluation of typical meteorological data (TMY3). Retrieved from <http://locusenergy.com/wp-content/uploads/2013/10/How-Typical-is-Solar-Energy-A-6-Year-Evaluation-of-TMY3-Locus-Energy-White-Paper.pdf>

Acknowledgements

This research was supported in part by grants from the NPS Acquisition Research Program and the Marine Corps Expeditionary Energy Office.





ACQUISITION RESEARCH PROGRAM
GRADUATE SCHOOL OF BUSINESS & PUBLIC POLICY
NAVAL POSTGRADUATE SCHOOL
555 DYER ROAD, INGERSOLL HALL
MONTEREY, CA 93943

www.acquisitionresearch.net